

1 diffraction (Rigaku SmartLab 9 kW). The fluorescence and phosphorescence spectra
2 were recorded by FL970 and FLS980, respectively. The absolute fluorescence quantum
3 yield was obtained by a calibrated integrating sphere in FLS980 spectrometer, and
4 fluorescence and phosphorescence lifetimes were characterized using FLS980 time-
5 corrected single photon counter system.

6 **Synthesis of PCN**

7 Preparation of S, N-PCN, and N-PCN: 0.6g thiourea were uniformly ground in a mortar
8 for 5 min, and then transferred to a 50 mL autoclave for heating at 260 °C for 12 h. Then
9 take out the autoclave, after it cool down to room temperature naturally. After drying
10 the powder at 40 °C, continue grinding for sample characterization. All conditions for
11 S, N-PCN0 synthesis are the same as described above, except that thiourea was
12 transferred to a beaker wrapped in tin foil. All conditions for N-PCN synthesis are the
13 same as described S, N-PCN, except that the thiourea was replaced by urea.

14 Preparation of S, N-PCN0: 0.6g thiourea were uniformly ground in a mortar for 5 min,
15 and then transferred to a 50 mL autoclave for heating at 260 °C for 12 h. Then take out
16 the beaker, after it cool down to room temperature naturally. After drying the powder
17 at 40 °C, continue grinding for sample characterization. The obvious difference from
18 S, N-PCN, prepared S, N-PCN0 is an open reaction environment.

19 Preparation of thiourea :urea (4:1), thiourea :urea (1:1) thiourea :urea (1:4)
20 thiourea :urea (1:16): thiourea and urea (mass ratio = 4:1, 1:1, 1:4, 1:16) were uniformly
21 ground in a mortar for 5 min, and then transferred to a 50 mL autoclave for heating at
22 260°C for 12 h. Then take out the autoclave, after it cool down to room temperature

1 naturally. After drying the powder at 40 °C, continue grinding for sample
2 characterization.

3 **Facilitating ISC rule**

4 Accordingly, the phosphorescence efficiency (Φ_P) and lifetime (τ_P) can be
5 expressed as¹⁻⁴:

$$6 \quad \Phi_P = \Phi_{ISC}[1 - (k_{nr} + k_q)]\tau_P \quad (1)$$

$$7 \quad \Phi_{ISC} = \frac{k_{ISC}}{k_F + k_{IC} + k_{ISC}} \quad (2)$$

$$8 \quad \tau_P = \frac{1}{k_P + k_{nr} + k_q} \quad (3)$$

9 where Φ_{ISC} is the quantum yield of ISC, and k represents the transition rate related
10 to each process: k_F is the fluorescent decay rate, k_{IC} the internal conversion (IC) rate
11 from S_1 to S_0 , k_{ISC} the ISC rate from S_1 to T_n , k_P the phosphorescent decay rate, k_{nr} the
12 triplet non-radiative decay rate and k_q the overall quenching rate of T_1 after integrating
13 the concentration of quenchers. ISC is the critical process for populating triplet excitons
14 and, thus, determines the upper limit of Φ_P (Eq. (1)). According to Eq. (2), organic
15 phosphors with an ISC rate (k_{ISC}) fast enough ($<10^{11} \text{ s}^{-1}$) to compete with the
16 fluorescent decay rate (k_F , $\sim 10^7$ - 10^{10} s^{-1}) and the internal conversion rate (k_{IC} , $<10^{11}$
17 s^{-1}) can have a high yield of ISC (Φ_{ISC}). k_{ISC} is an intrinsic feature of organic molecules
18 and it mostly depends on the electronic configuration and energy levels, which can be
19 expressed as^{5,6}:

$$20 \quad k_{ISC} = \frac{2\pi}{\hbar} |\langle S | \hat{H}_{soc} | T \rangle|^2 \sqrt{\frac{\pi}{\lambda k_B T}} \exp\left[-\frac{(\Delta E_{ST} - \lambda)^2}{4\lambda k_B T}\right] \quad (4)$$

21 where $\langle S | \hat{H}_{soc} | T \rangle$ is the spin-orbit coupling (SOC) matrix element between singlet

1 and triplet states, \hbar is the reduced Planck's constant, λ is the total reorganization
 2 energy, k_B is the Boltzmann constant, T is the temperature and ΔE_{ST} represents the
 3 energy gap between the involved singlet and triplet states at their equilibrium
 4 geometries. Based on Eq. (4), the principles can guide the design of systems with
 5 improved ISC and provide some examples of PCN materials to facilitate the ISC
 6 process. It is reported, from a mechanistic perspective, tuning of the molecular orbital
 7 configurations based on the El-Sayed rule, reductions of the energy gap ΔE_{ST} could
 8 facilitate the process of ISC, which enables the production of more triplet excitons
 9 through energy transfer⁵.

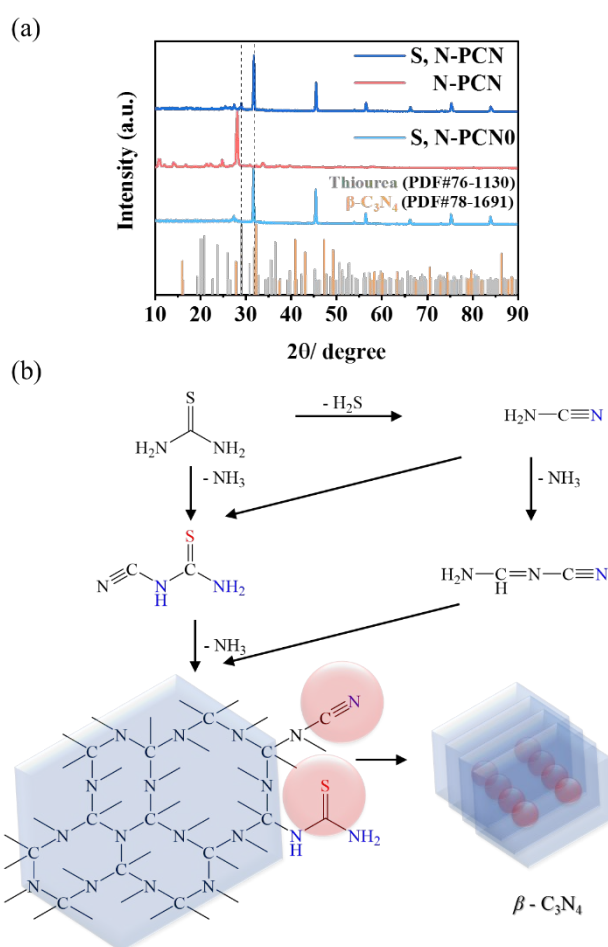


Figure S1. (a) XRD survey spectra of S, N-PCN0, S, N-PCN, and N-PCN. (b) Possible structure
 S4

for self-polymerization of thiourea to the polymeric carbon nitride at low temperature. The reaction process is simplified.

Polymerization inevitably has some degrees in difference of size and crystal structure. In Figure S1(a) PCN shows a tiny peak at 27.4° , corresponding to the heptazine heterocyclic ring units⁷. It means the formation of polycrystalline compounds (β - C_3N_4 and g - C_3N_4), but it is main composed of β - C_3N_4 . β - C_3N_4 has similar structure to β - Si_3N_4 , which is substituted for Si with C in the β - Si_3N_4 structure⁸. In Figure S1(b), it shows the possible routes of reaction involving intermediates and final products. Due to the incomplete reaction, intermediate products may be involved in the reaction, which leads to the presence of special S, and N elements⁹.

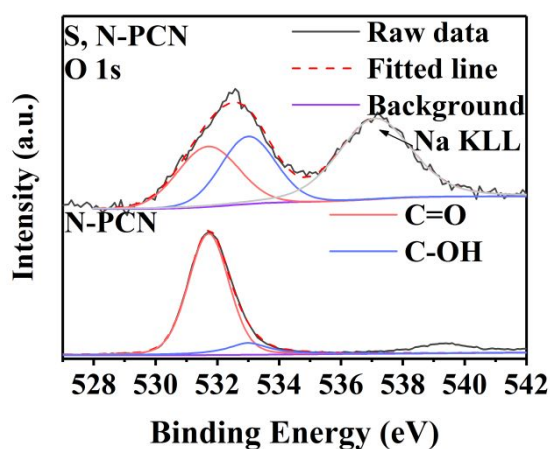


Figure S2. XPS fitting results of O 1s for S, N-PCN and N-PCN.

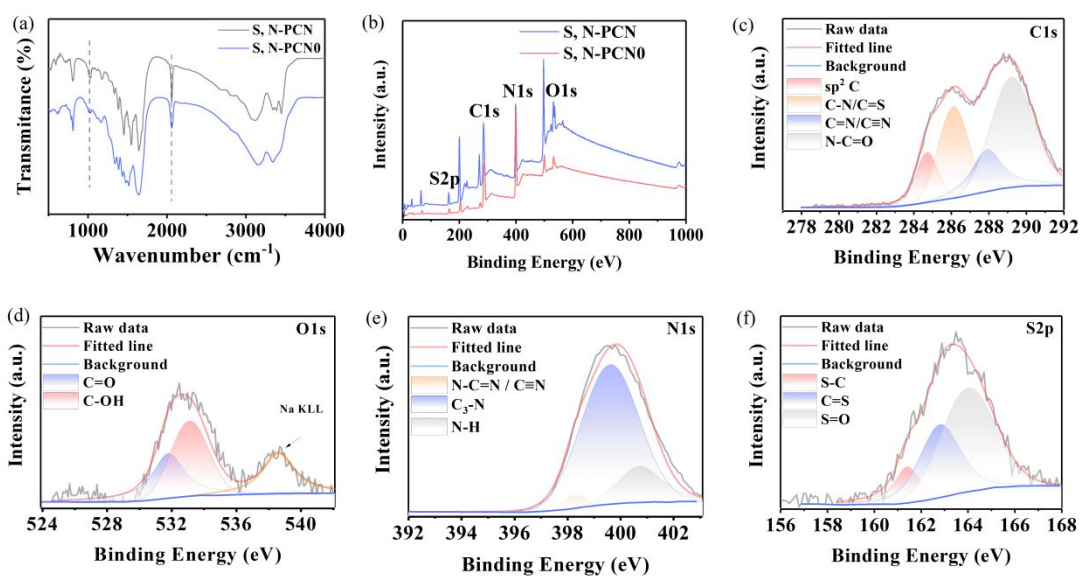


Figure S3. (a) FT-IR spectra of S, N-PCN and S, N-PCN0. (b) XPS spectra of S, N-PCN and S, N-PCN0. XPS fitting results of (c) C 1s, (d) O 1s (e) N 1s, and (f) S 2p for S, N-PCN0.

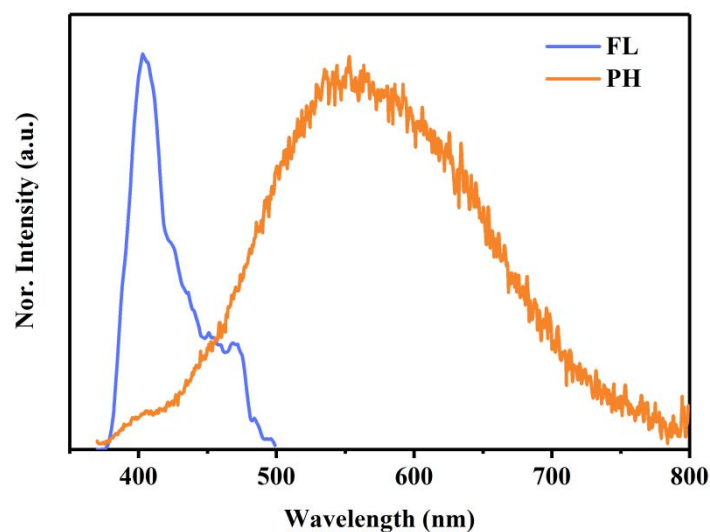


Figure S4. FL emission (blue line) and corresponding phosphorescence emission (orange line) spectra of the S N-PCN0.

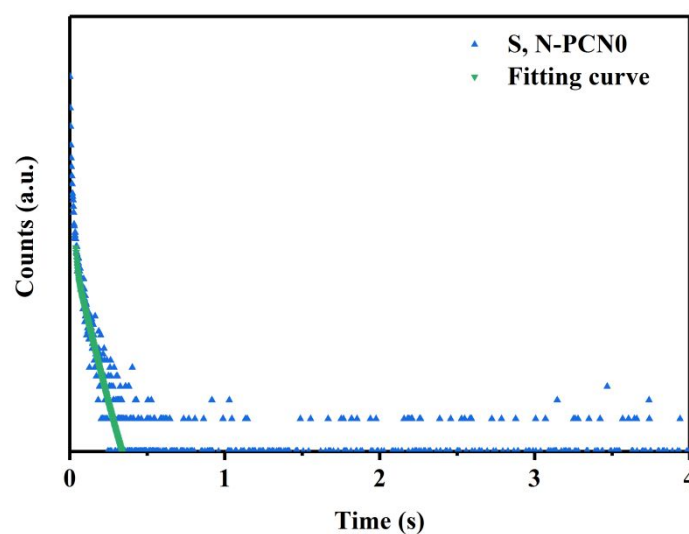


Figure S5. Phosphorescence decay spectrum and fitting curve S, N-PCN0 under ambient conditions.

Apparently, the major difference between S, N-PCN and S, N-PCN0 is that S, N-PCN displays a stronger XPS and FT-IR signal at higher content of C=S and C≡N groups, indicating the S and N elements play a key role in RTP. Since C=S and C≡N groups in the networks, it influences FL emission assigned to the $n-\pi^*$ transition^{10,11}. The S, N-PCN0 shows the fluorescence at 403 nm and phosphorescence at 553 nm (Figure S4). In Figure S5, the RTP decay spectrum of the S, N-PCN0 is fitted by a triexponential function and shows an average lifetime of 72.3 ms ($\lambda_{\text{ex}} = 360$ nm, $\lambda_{\text{em}} = 553$ nm). From N 1s, O 1s, and S 2p spectra, it's worth noting that S, N-PCN shows the increase of related RTP functional groups (C=S and C≡N), which may play an important role in RTP emission.

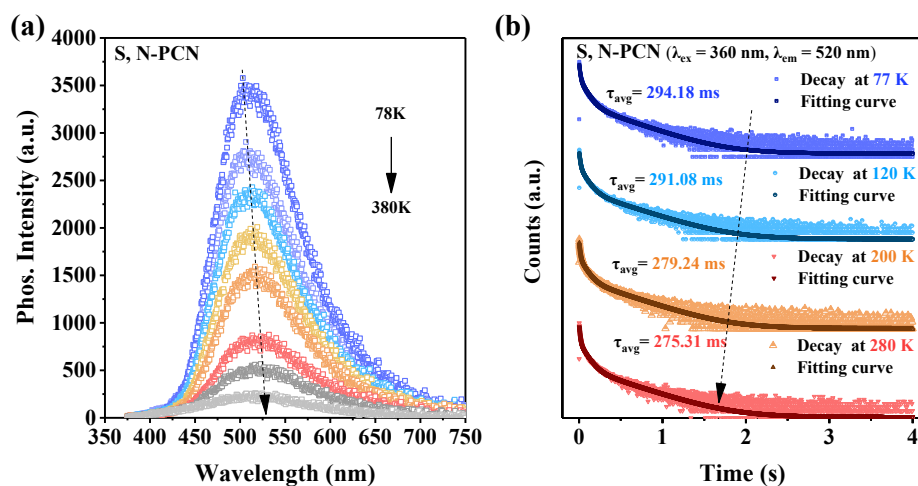


Figure S6. (a) Phosphorescence and (b) phosphorescence decay spectra of S, N-PCN under the excitation 360 nm (λ_{em} = 515 nm) from 78K to 380K.

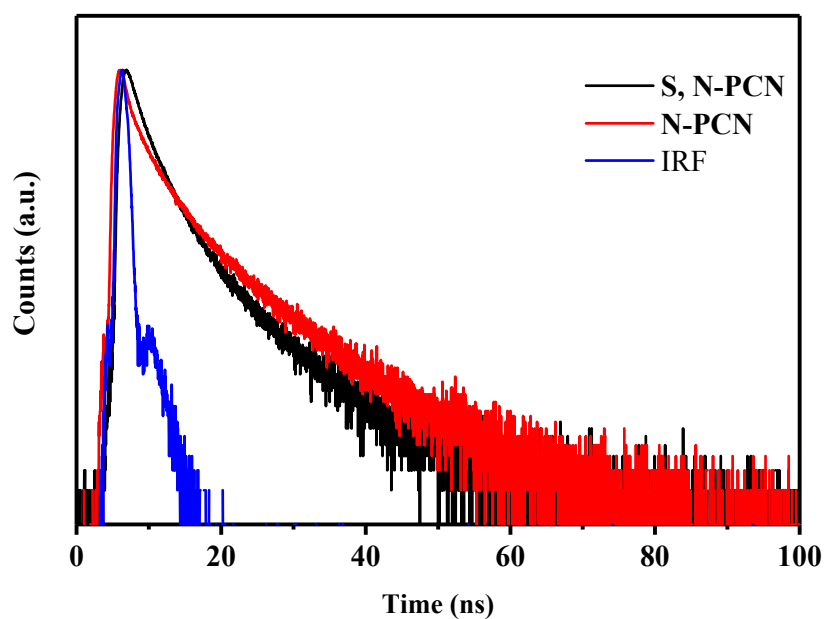


Figure S7. FI decay spectra and IRF of S, N-PCN (λ_{ex} = 405 nm, λ_{em} = 480 nm) and N-PCN (λ_{ex} = 405 nm, λ_{em} = 430 nm).

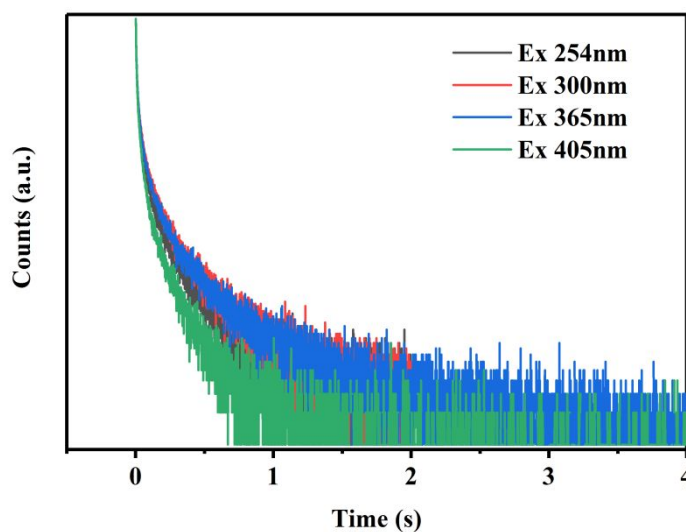
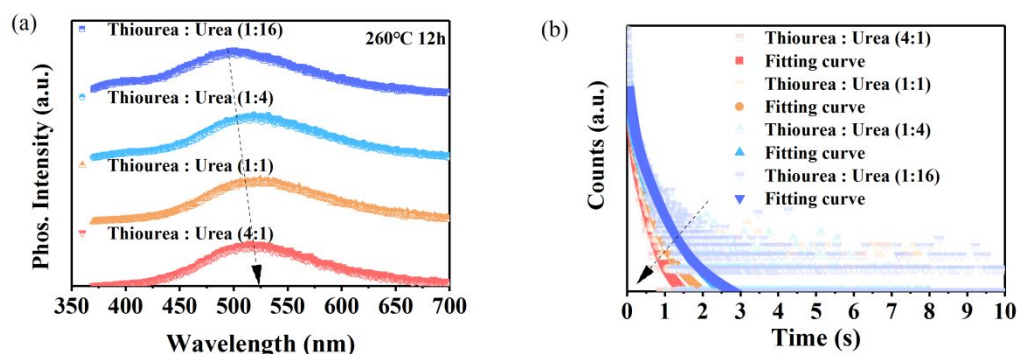


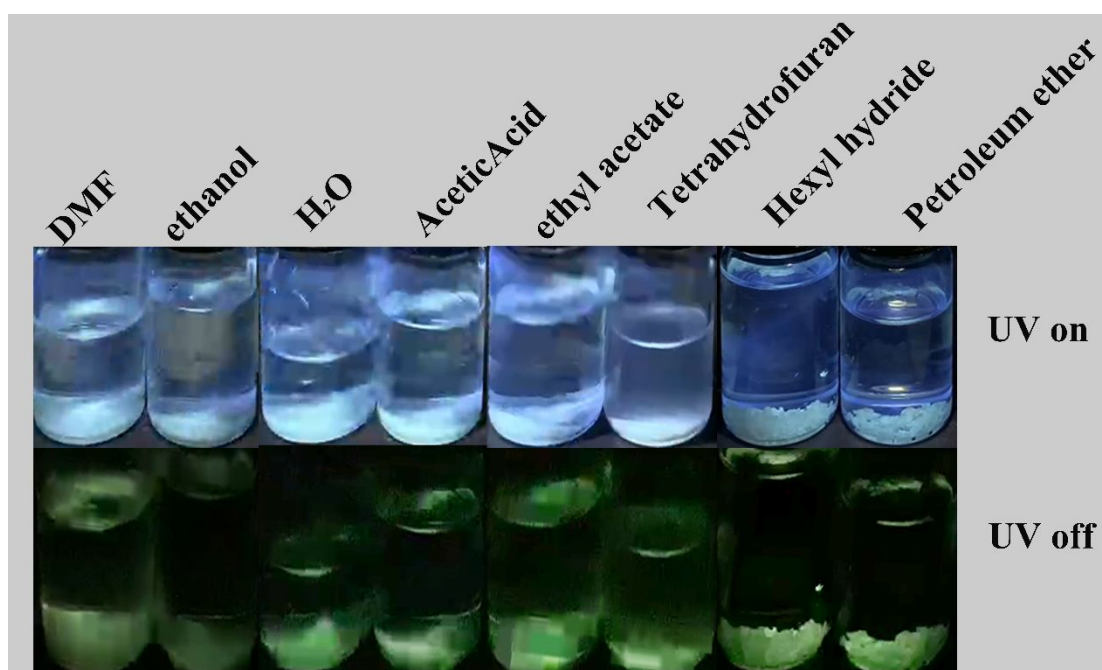
Figure S8. Phosphorescence decay spectra of S, N-PCN under the excitation of 254, 300, 365, 405 nm ($\lambda_{em}=515$ nm).

Furthermore, the phosphorescence spectrum of S, N-PCN from 78 K to 380 K shows a bit redshift, indicating a typical feature for energy transfer in these emission centers^{12,13} (Figure S6). The time-resolved fluorescence spectra of S, N-PCN and N-PCN were also fitted with a tri-exponential function with an average lifetime of 4.69 and 5.58 ns, respectively (Figure S7). The introduction of C=S and C≡N groups in S, N-PCN networks firmly promotes the ISC from singlet to triplet states and then leading to highly efficient phosphorescence, which was further confirmed by a faster ISC rate, k_{ISC} , (8.8×10^6 s⁻¹) for S, N-PCN than those for N-PCN (7.2×10^5 s⁻¹) (Table S5). Furthermore, it was found that S, N-PCN showed a faster radiative transition, k_r^P , (1.4×10^{-1} s⁻¹) and slower nonradiative decay rates (5.5×10^{-3} s⁻¹) compared with those for N-PCN (Table S5). Moreover, the lifetimes S, N-PCN were obtained 201.7, 221.4, 291.1 and 125.2 ms by monitoring RTP emission at 515 nm following excitation at 254,

1 300, 365, 405 nm, respectively (Figure S8). These results further suggest that the S, N-
 2 PCN exists multiple emission centers.



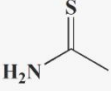
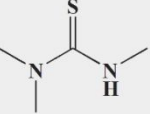
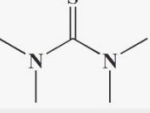
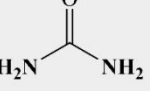
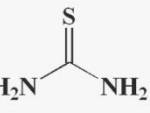
3
 4
 5 Figure S9. (a) The red-shift phosphorescence spectra of different mole ratios of thiourea and urea
 6 from 1:16 to 4:1 at 260 °C 12h. (b) Phosphorescence decay spectrum of S, N-PCN under
 7 the excitation of 360 nm ($\lambda_{em}=515$ nm).
 8



9
 10
 11 Figure S10. Photographs of S, N-PCN in polar solvents under UV on and off.
 12

13 In order to further investigate the extraordinary stability of S, N-PCN, it was
 14 dispersed in different polar solvents. It was found that the phosphors also maintained
 15 superior stability in organic polar solvents (Figure S10).
 16

Table S1. Summary of PQY and the RTP properties of polymers prepared by different precursors at 260 °C (12 h)

Chemical Name	Structural Formula	PQY	RTP
Thioacetamide		×	×
Trimethylthiourea		×	×
Tetramethylthiourea		×	×
Urea		✓	✓
Thiourea		✓	✓

To confirm the relationship between the structural properties of polymers and RTP properties, a variety of thiourea analogues (Thioacetamide, Trimethylthiourea, Tetramethylthiourea) was selected to carry out contrast experiments. It was synthesized under the same temperature and heating time, for purpose of the accuracy of comparison (Table S1). Unfortunately, three types of thiourea analogues had no FL or RTP emission. Interestingly, the phenomenon of FL and RTP emission for urea and tiourea was discovered.

Table S2. Element analysis of S, N-PCN, S, N-PCN0, and S, N-PCN.

Samples	C 1s	N 1s	O 1s	S 2p
S, N-PCN	51.27%	31.46%	13.72%	3.55%
S, N-PCN0	50.05%	42.35%	5.68%	1.92%
N-PCN	39.80%	44.40%	15.8%	0%

Table S3. Content of various chemical bonds in S, N-PCN, S, N-PCN0, and N-PCN respectively

Samples	C 1s					N 1s		S 2p			O 1s	
	sp ² C	C-N/C=S	C=N/C≡N	N-C=O	N-C=N/C≡N	(C) ₃ -N	N-H	C-S	C=S	S=O	C=O	C-OH
	283.5 eV	285.1 eV	286.9 eV	288.1 eV	398.3 eV	399.6 eV	400.7 eV	163.7 eV	164.9 eV	164.2 eV	531.7 eV	533.1 eV
S, N-PCN	29.21%	41.07%	15.79%	13.93%	35.31%	52.07%	12.62%	75.20%	22.70%	2.10%	48.75%	51.25%
S, N-PCN0	10.73%	31.82%	10.29%	47.16%	3.33%	76.48%	20.19%	53.80%	15.31%	30.89%	43.58%	56.42%
N-PCN	15.69%	3.54%	26.32%	54.45%	3.36%	74.57%	21.76%	/	/	/	87.83%	12.17%

Table S4. Fitting parameters of the corresponding phosphorescence decay curve of the corresponding S, N-PCN, N-PCN, S, N-PCN0, and thiourea : urea.for the ratio of 1:16, 1:4, 1:1, and 4:1.

Samples	τ_1 (ms)	τ_2 (ms)	τ_3 (ms)	A_1 (%)	A_2 (%)	A_3 (%)	$\tau_{avg.}$ (ms)
S, N-PCN (Ex254 nm)	5.66	39.59	241.03	25.17	42.83	32	201.75
S, N-PCN (Ex300 nm)	5.76	46.59	260.8	20.5	42.94	36.56	221.44
S, N-PCN (Ex360 nm)	7.68	61.97	358.59	27.57	44.09	28.34	291.08
S, N-PCN (Ex405 nm)	4.79	28.69	159.95	26.66	47.08	26.26	125.23
S, N-PCN (80 K; Ex360 nm)	10.00	65.44	363.13	26.94	48.02	25.04	280.71
S, N-PCN (120 K; Ex360 nm)	10.00	64.06	355.34	25.79	48.52	25.69	275.75
S, N-PCN (200 K; Ex360 nm)	09.62	62.40	348.88	27.84	45.72	26.44	275.31
N-PCN (Ex360 nm)	10.00	100	773.89	4.59	24.08	71.33	745.13
S, N-PCN0 (Ex360 nm)	10.00	73.33	0	10.10	89.90	0	72.37
thiourea :urea (1:16)	73.85	298.7	1257.22	33.68	55.6	10.72	678.13
thiourea :urea (1:4)	53.47	212.91	907.97	35.17	54.27	10.56	489.34
thiourea :urea (1:1)	41.07	175.42	688.58	21.00	54.96	24.04	485.08
thiourea :urea (4:1)	44.60	187.46	877.56	35.25	55.89	08.86	446.78

Table S5. Dynamic photophysical parameters of S, N-PCN and N-PCN.

Materials	Φ_P (%)	τ_F (ns)	τ_P (s)	k_{ISC} (s ⁻¹) ⁽⁵⁾	k_r^P (s ⁻¹) ⁽⁶⁾
S, N-PCN	4.15	4.69	0.29	8.8×10^6	1.4×10^{-1}
N-PCN	0.41	5.58	0.74	7.2×10^5	5.5×10^{-3}

$$k_{ISC} = \frac{\Phi_P}{\tau_F} \quad (5)$$

$$k_r^P = \frac{\Phi_P}{\tau_P} \quad (6)$$

Reference

- (1) Hirata, S.; Totani, K.; Zhang, J.; Yamashita, T.; Kaji, H.; Marder, S. R.; Watanabe, T.; Adachi, C. Efficient Persistent Room Temperature Phosphorescence in Organic Amorphous Materials under Ambient Conditions. *Adv. Funct. Mater.* **2013**, *23*, 3386-3397.
- (2) Ma, X.; Xu, C.; Wang, J.; Tian, H. Amorphous Pure Organic Polymers for Heavy-Atom-Free Efficient Room-Temperature Phosphorescence Emission. *Angew Chem Int Ed Engl* **2018**, *57*, 10854-10858.
- (3) Zhao, W.; Cheung, T. S.; Jiang, N.; Huang, W.; Lam, J. W. Y.; Zhang, X.; He, Z.; Tang, B. Z. Boosting the efficiency of organic persistent room-temperature phosphorescence by intramolecular triplet-triplet energy transfer. *Nat Commun* **2019**, *10*, 1595.
- (4) Bian, L.; Shi, H.; Wang, X.; Ling, K.; Ma, H.; Li, M.; Cheng, Z.; Ma, C.; Cai, S.; Wu, Q.; Gan, N.; Xu, X.; An, Z.; Huang, W. Simultaneously Enhancing Efficiency and Lifetime of Ultralong Organic Phosphorescence Materials by Molecular Self-Assembly. *J. Am. Chem. Soc.* **2018**, *140*, 10734-10739.
- (5) Zhao, W.; He, Z.; Tang, B. Z. Room-Temperature Phosphorescence from Organic Aggregates. *Nat. Rev. Mater.* **2020**, *5*, 869-885.
- (6) Penfold, T. J.; Gindensperger, E.; Daniel, C.; Marian, C. M. Spin-Vibronic Mechanism for Intersystem Crossing. *Chem. Rev.* **2018**, *118*, 6975-7025.
- (7) Zhang, G.; Zhang, J.; Zhang, M.; Wang, X. Polycondensation of thiourea into carbon nitride semiconductors as visible light photocatalysts. *J. Mater. Chem.* **2012**, *22*, 8083.

- (8) Liu, A. Y.; Cohen, M. L. Structural properties and electronic structure of low-compressibility materials: β -Si₃N₄ and hypothetical β -C₃N₄. *Phys. Rev. B* **1990**, *41*, 10727-10734.
- (9) Li, Y.; Jin, S.; Xu, X.; Wang, H.; Zhang, X. Excitonic effects on photophysical processes of polymeric carbon nitride. *J. Appl. Phys.* **2020**, *127*,
- (10) Gao, D.; Zhang, Y.; Liu, A.; Zhu, Y.; Chen, S.; Wei, D.; Sun, J.; Guo, Z.; Fan, H. Photoluminescence-Tunable Carbon Dots from Synergy Effect of Sulfur Doping and Water Engineering. *Chem. Eng. J.* **2020**, *388*, 124199.
- (11) Yang, H.; Liu, Y.; Guo, Z.; Lei, B.; Zhuang, J.; Zhang, X.; Liu, Z.; Hu, C. Hydrophobic carbon dots with blue dispersed emission and red aggregation-induced emission. *Nat Commun* **2019**, *10*, 1789.
- (12) Wong, C. Y.; Alvey, R. M.; Turner, D. B.; Wilk, K. E.; Bryant, D. A.; Curmi, P. M. G.; Silbey, R. J.; Scholes, G. D. Electronic coherence lineshapes reveal hidden excitonic correlations in photosynthetic light harvesting. *Nat. Chem.* **2012**, *4*, 396-404.
- (13) Dias, F. B.; Bourdakos, K. N.; Jankus, V.; Moss, K. C.; Kamtekar, K. T.; Bhalla, V.; Santos, J.; Bryce, M. R.; Monkman, A. P. Triplet harvesting with 100% efficiency by way of thermally activated delayed fluorescence in charge transfer OLED emitters. *Adv. Mater.* **2013**, *25*, 3707-3714.